A narrow bandwidth detection method for inter-harmonics in Tokamak power supply

Yunxiang Tian[1,2], Liuwei Xu[1], Jing Lu[1], Yanan Wu[1]
1. Institute of Plasma Physics
Chinese Academy of Sciences
2. University of Science and Technology of China
Hefei, China
yunxiang.tian@ipp.ac.cn, xulw@ipp.ac.cn,
lujing@ipp.ac.cn, wyn@ipp.ac.cn

Junmin Zhang
Department of Computer Science
South-Center University for Nationalities
Wuhan, China
173902815@qq.com

***Abstract*—Low-frequency harmonics which are close to the fundamental have characteristics of small amplitude and non-stationary state, and contain complex side-lobe inter-harmonics. To ensure the precise and real-time extraction of the whole spectrum band, the compensation measure is difficult. In order to solve this detection problem, a hybrid detection algorithm is proposed based on elliptic digital bandpass filter with boundary characteristics and single-frequency notch filter with optimal Q-factors, which can effectively extract the according band. Single-frequency notch filter has excellent third-order harmonic suppression ability and dynamic robustness characteristics. Elliptic digital bandpass filter can extract harmonics of target frequency band and ensure the phase offset, so as to achieve effective spectrum separation. Simulation with MATLAB is adopted to improve the design process. The validity of the detection algorithm is verified by experiments with digital analysis system based on DSP.**

***Index Terms*--harmonic suppression; single-frequency notch filter; elliptic digital bandpass filter; low-frequency harmonics.**

I. INTRODUCTION

In recent years, although the Experimental Advanced Superconducting Tokamak (EAST) made in China has acquired a series of great achievements in the research of controllable nuclear fusion and provided a great guiding significance to the construction and operation of the International Thermonuclear Experimental Reactor (ITER). However, the power supply has gradually become the source of some non-characteristic harmonics with abundant side-lobes, especially the low-order inter-harmonics. Furthermore, capacitive branch of reactive power compensation forms resonance accompanied with the reactor on the grid side, which endangers the safety of the whole system [1], [2]. The whole system is shown as Fig.1.

As the starting point of harnessing harmonic pollution, harmonic detection has become an important research object for scholars. The harmonic current detection based on instantaneous reactive power theory and adaptive detection method effectively extracts the fundamental signal which is used to subtract the grid signal, and then the compensation signal is obtained [3]-[6]. The methods are widely used because of their remarkable effects on the extraction of fixed-frequency signal, however, the problem of signal extraction in a certain frequency band cannot be solved. Wavelet analysis method has better time-frequency characteristics, which can availably detect abrupt harmonics and obtain more accurate harmonic parameters. However, the application is limited due to long sampling time, difficult selection of wavelet bases and ineffective separation of similar frequencies [7], [8]. Considering the dynamic and steady state characteristics of the whole system, the background and method of harmonic detection are introduced.

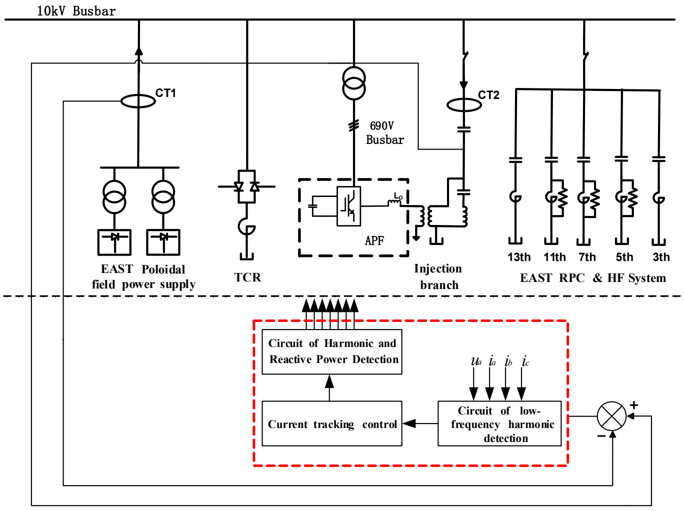

Figure 1. EAST poloidal power supply system.

II. PRINCIPLES

The typical phenomenon of second-harmonic emission from poloidal field power supply is revealed by analyzing a large number of operation data of harmonics in poloidal field during EAST experiment, as shown in Fig.2. The frequency and amplitude of inter-harmonics emitted by

This work was supported in part by the NSFC (National Science Foundation of China) under Grant 51707190 and Key R&D Program of Anhui Province under Grant 201904a05020090. (Corresponding author: Jing Lu.)

converters under typical operating conditions are shown in Fig.3.

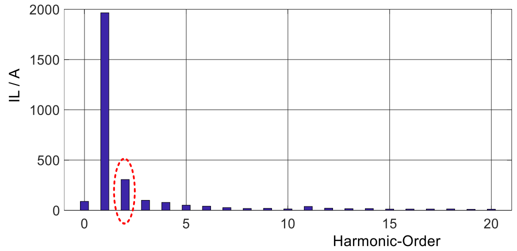

Figure 2. Harmonic current of converter.

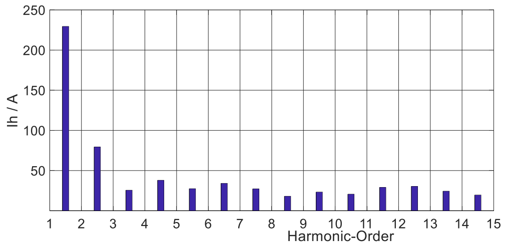

Figure 3. Typical emission phenomena of inter-harmonics.

As can be seen from Fig. 1 and Fig. 2, the second harmonic and its adjacent inter-harmonic have larger amplitude and are quite close to the fundamental frequency, which brings large difficulties to the restraining process. Therefore, the research object of this paper is to control the inter-harmonic near the fundamental wave, for convenience of the research, low-frequency harmonics are defined as signals with the frequency range between 75Hz and 125Hz.

Due to the signal transition band is narrow and the fundamental current is of large amplitude to 2kA, the design of traditional filters is challenged [9]. Considering the harmonic capacity of EAST, ITER and other devices, APF (Active Power Filter) cannot be used to achieve full-band harmonic control. How to effectively compensate low-band harmonics and inter-harmonics is a problem to be solved. Since the signal to be extracted is the harmonic of a certain frequency band and the inter-lobe harmonic, how to guarantee the efficacious compensation of APF from the phase offset is another urgent problem to be considered [10], [11]. In the design process of digital filter, the high attenuation of amplitude will result in the high order of function, which causes the design difficult to realize in engineering. Moreover, the signal changes rapidly and dramatically, so the real-time performance of the treatment process is particularly important.

Aiming at the questions mentioned above, the requirements of the detection system should be analyzed.

1) In order to extract the low-frequency harmonics, a passband filter needs to be designed. Since the narrower the bandwidth of the filter is, the more complex the detection system is, appropriately increasing the bandwidth is necessary.

2) When the phase difference between APF output signal and grid signal is between -90° and +90°, the compensation effect is achieved. Therefore, to ensure that the phase of 75~125 Hz signal is within the range is necessary, and considering the delay characteristics of APF itself, the phase of the filter should be controlled between -60° and +90°.

3) To avoid the third harmonics inrush because of the increase of bandwidth, the 3rd-order harmonics need to be suppressed at the same time.

Therefore, a comprehensive detection algorithm of harmonic extraction is needed to meet the above requirements.

III. Detection Algorithm

A. Optimum design of passband filter boundary

To extract the second harmonics and its inter-harmonics submerged in high amplitude fundamental-frequency signals, it is necessary to design reasonable boundaries of pass, stop and transition bands, and to establish an improved amplitude-phase model combined with different compensation requirements.

For filters, the maximum attenuation of passband R_p, the minimum attenuation of stopband R_s, the boundary frequency of passband ω_p and the cut-off frequency of stopband ω_s are the four key factors in the design process by (1) and (2).

$$\omega_p = 2*\left[(\varepsilon_1+\Delta\sigma_1),(\varepsilon_2+\Delta\sigma_2)\right]/F_s \tag{1}$$

$$\omega_s = 2*\left[(\varepsilon_1+\Delta\sigma_3),(\varepsilon_2+\Delta\sigma_4)\right]/F_s \tag{2}$$

Where F_s denotes sampling frequency and F_s=3200Hz ; ε_1 denotes the left boundary frequency of passband; ε_2 denotes the right boundary frequency of passband; $\Delta\sigma_i$ denotes adjustable frequency.

In engineering design, the maximum attenuation of passband and the minimum attenuation of stopband are generally set to 3dB and 30dB, respectively, that is:

$$R_p = 3dB \tag{3}$$

$$R_s = 30dB \tag{4}$$

According to analysis of detection system and the zero-crossing characteristic of the filter used to suppress the fundamental and the 5th harmonics, ε_1 and ε_2 can be set to the values as follows:

$$\begin{cases}\varepsilon_1 = 50Hz \\ \varepsilon_2 = 250Hz\end{cases} \tag{5}$$

Considering that the larger the order N of the filter is, the more difficult the expected effect of the whole system is to be achieved, therefore in this paper, the value of N is no more than 7:

$$N \le 7 \tag{6}$$

Considering that the frequency band needed to be extracted is close to the second harmonic, by iterative operation of (1)-(6), the optimum solution can be obtained as (7), as shown in Fig.4.

$$\begin{cases}\omega_p = 2*\left[66.1,190\right]/3200 \\ \omega_s = 2*\left[0.1,250\right]/3200\end{cases} \tag{7}$$

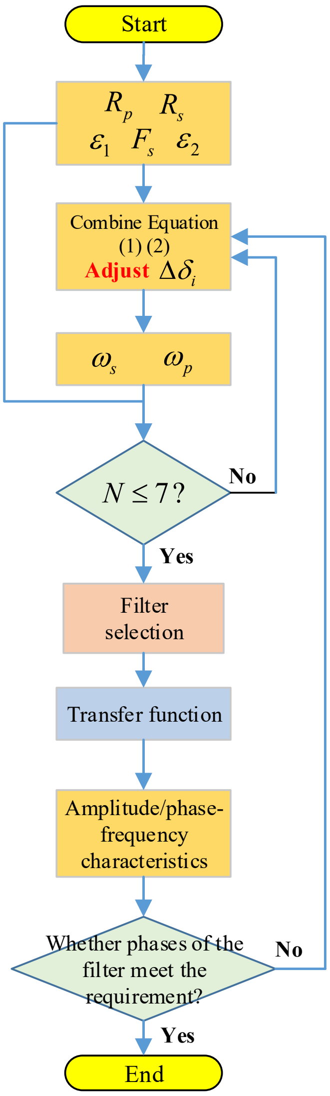

Figure 4. Iterative operation of determining parameters.

Common types of digital filters are Butterworth, Chebyshev and elliptic filters. Since Butterworth and type-I Chebyshev filters cannot meet the phase requirements of this design (between -60° and +90°), and elliptic filters are equal ripple approximation in passband and stopband, of which approximate characteristics of passband and stopband are excellent. For the same performance requirement, the order of elliptic filter is lower than that of type-II Chebyshev filter, and the transition band is narrower. Therefore, the elliptic digital bandpass filter is chosen in this design [12], [13].

And according to functions of ellipord, the transfer function of elliptic filter is obtained as follows:

$$H(z)=\frac{\sum_{i=0}^{6} b_i z^{-i}}{1+\sum_{j=1}^{6} a_j z^{-j}} \tag{8}$$

Where the coefficients of denominator polynomial and numerator polynomial are respectively shown as Table 1.

TABLE I. COEFFICIENTS OF TRANSFER FUNCTION

$a_i\,(i=0,1,\cdots$	$b_j\,(j=0,1,\cdots$
1	0.0138929
-5.6705687	-0.0521682
13.5754119	0.0626892
-17.5600790	0
12.9436131	-0.0626892
-5.1551689	0.0521682
0.8668964	-0.0138929

Through the simulation, the amplitude/phase-frequency characteristics of the elliptic digital bandpass filter are shown in Fig.5.

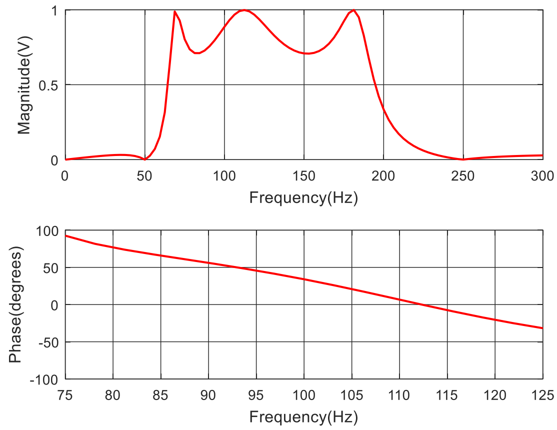

Figure 5. Amplitude/Phase-frequency characteristics of elliptic filter.

B. Notch filter based on optimal Q-factors

Owing to the large amplitude of the third harmonic in the passband frequency, it is necessary to adopt effective filtering methods. Notch filter is equivalent to a band-stop filter which can be used to filter out the harmonic components with a specific frequency. Thus, notch filter has good effect in suppressing single-frequency interference without influencing the control performance of other frequency bands.

The typical transfer function of the second-order Q-factors notch filter is expressed as

$$G(s)=A_0\frac{s^2+\omega_n^2}{s^2+\omega_n s/Q+\omega_n^2} \tag{9}$$

Where A_0 denotes the gain of the filter, generally $A_0 = 1$; ω_n is characteristic angular frequency; Q denotes the equivalent quality factor, showing the frequency selection performance of notch filter. The larger the value of Q, the narrower the transition band, that is, the better the notch effect, but the longer the delay time, the worse the dynamic response performance [14], [15].

The signal changed rapidly and violently, therefore, it needs to be compensated in two cycles of fundamental. Considering that the delay time of digital filter is very short, the delay time of notch filter circuit should be controlled in two cycles, that is, 0.04s. Due to the increase of the quality factor of notch filter will lead to the increase of delay time, and the dynamic response delay will exceed 0.04s after Q exceeds 10, so the situations are simulated when the value of Q is 5, 8 and 10, respectively. When $\omega_n = 2\pi f_n = 300\pi$, $A_0 = 1$, the amplitude/Phase-frequency characteristics and dynamic response process of the notch filter under MATLAB simulation environment are shown in Fig.5 and Fig.6 when the quality factor values are 5, 8 and 10, respectively.

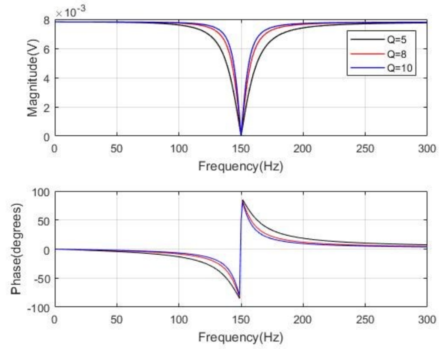

Figure 6. Amplitude/Phase-frequency characteristics.

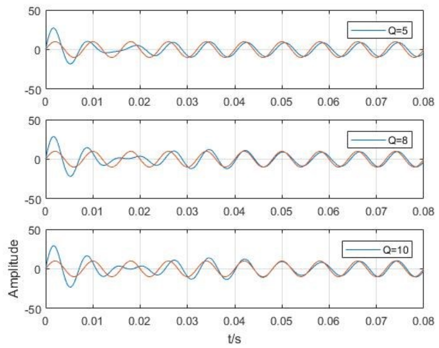

Figure 7. Dynamic response (MATLAB simulation).

From Fig.6, the attenuation of signal amplitude at characteristic frequency 150Hz (the third harmonics) is as high as -125dB, which means that the amplitude of third harmonics can be attenuated to approximately 0. And as the quality factor increases, the transition band is narrower and the notch effect becomes better, on the other hand, the delay time is longer, which means that the dynamic response performance becomes worse. Comprehensively considering, the notch filter circuit with Q as 8 will be selected. And equation (9) can be expressed by (10).

$$G(s) = \frac{s^2 + (2\pi \times 150)^2}{s^2 + (2\pi \times 150)s/8 + (2\pi \times 150)^2} \tag{10}$$

IV. EXPERIMENTAL VERIFICATION

A. Elliptic digital bandpass filter

In order to verify the effectiveness of elliptic digital filter, a DSP digital analysis system based on TMS320F2812 is designed. Three cases in the experiment are shown in Fig.8, the green line is the input signal (sine wave) and the purple line is the output wave through DSP with algorithm of the elliptic filter. And the peak value of the input signal in this design is 2V. And the results of the treatment are shown in Table 2.

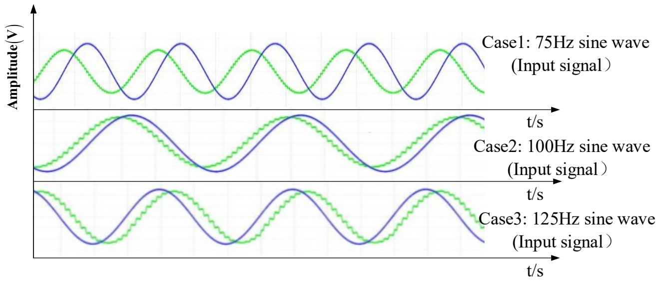

Figure 8. Output waveform of the elliptic digital filter.

TABLE II. AMPLITUDE AND PHASE VALUE OF CHARACTERISTIC SIGNALS AMONG TREATED SIGNALS

Frequency(Hz)	Amplitude(V)	Phase(degree)
75	0.781	86.92
100	0.892	30.23
125	0.952	-30.44

As is shown in Table 2, amplitudes of signals needed to be extracted satisfy the maximum attenuation (3dB), that is, amplitudes of the signals are above 0.707V. The phases of the signals also meet the design requirements. The results in Table 2 verifies the correctness of the design, and the signals mentioned in this design can be effectively extracted.

B. Analog notch filter

To further validate the design function of the notch filter, F42N150 analog notch filter is used with the same DSP digital analysis system. Compared with the notch filter made up of UAF42 of TI Company, F42N150 has smaller volume and fewer external components, which can adjust the quality factor directly by adjusting the external resistance.

In this experiment, the dynamic and steady state response performance of notch filter is verified by using sine wave signal of 75Hz and 125Hz as reference signals respectively. Testing experiments include steady-state and dynamic response performance testing, results of which when Q is 8 are shown in Fig.9 and Fig.10. The green line represents the output wave of mixed signal after the analog notch filter, and the purple line is the reference signal.

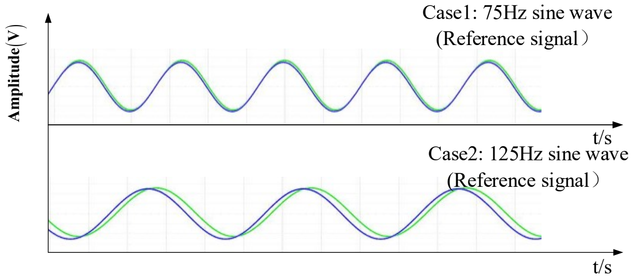

Figure 9. Static response.

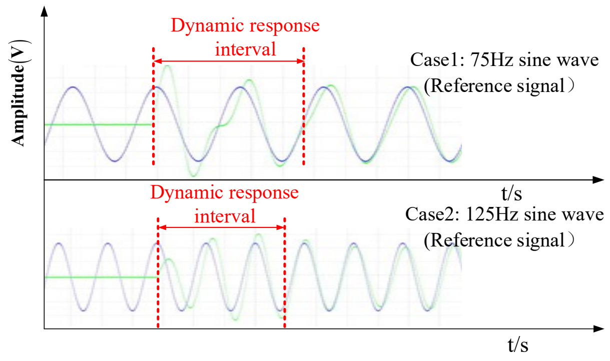

Figure 10. Dynamic response (Experiment).

Table 3 gives the performance of the analog notch filter from the experiment. The results are consistent to the prediction. Moreover, the third harmonics are disappeared in Fig.9 and Fig.10. The results test that the third harmonics are suppressed by the analog notch filter.

TABLE III. PERFORMANCE OF F42N150 NOTCH FILTER

Reference signal frequency	**Quality factor**	**Phase error of steady-state response**	**Delay of dynamic response**
75Hz	8	3.7°	20ms
125Hz	8	18.9°	20ms

V. CONCLUSIONS

A hybrid harmonic detection system based on elliptic digital bandpass filter and single-frequency notch filter is designed, which can effectively solve the continuous band detection problems of inter-harmonics. Meanwhile, the 3rd-order harmonics can also be suppressed to a low extent. The experimental results of the hybrid system reveal that the low-frequency harmonics near the fundamental can be well extracted, and the third harmonics can be attenuated to less than 1%, which fully verifies the correctness and effectiveness of the detection system.

REFERENCES

[1] Z Wang, J Yang, J Liu, *Harmonic Suppression and Reactive Power Compensation*, Beijing: China Machine Press, 2015.

[2] Y Wu, "Compatibility Analysis and Research on Tokamak Power and Reactive Power Compensation System with the Grid," Ph.D. dissertation, Beijing, China, University of Chinese Academy of Sciences, 2014.

[3] M. Y. Lada, S. S. Mohamad, J. Akbar, M. Gani, M. R. Nawawi, and E. Engineering, "Reduction of Harmonic Using Single Phase Shunt Active Power Filter based on Instantaneous Power Theory for Cascaded Multilevel Inverter," *2016 IEEE International Conference on Power and Energy (PECon)*, Melaka, 2016, pp. 702–706.

[4] F. Harirchi and M. G. Simões, "Enhanced Instantaneous Power Theory Decomposition for Power Quality Smart Converter Applications," *IEEE Transactions on Power Electronics*, vol. 33, no. 11, pp. 9344-9359, Nov. 2018.

[5] Z. Li, "Consistency Between Two Adaptive Detection Methods for Harmonic and Reactive Currents," *IEEE Transactions on Industrial Electronics*, vol. 58, no. 10, pp. 4981–4983, 2011.

[6] L. Guiyuan, X. Ziqiang, and L. Haowen, "An improved adaptive harmonic detection method applied in shunt APF," *2012 Power Engineering and Automation Conference*, Wuhan, 2012, pp. 1–4.

[7] Sugi R. and Sundararajan D., "Estimation of power quality indices using discrete wavelet transform," *2016 3rd International Conference on Advanced Computing and Communication Systems (ICACCS)*, Coimbatore, 2016, pp.1-5.

[8] J. Barros, S. Member, R. I. Diego, and M. De Apráiz, "Applications of Wavelet Transform for Analysis of Harmonic Distortion in Power Systems: A Review," *IEEE Transactions on Instrumentation and Measurement*, vol. 61, no. 10, pp. 2604 –2611, 2012.

[9] J Lu, P Fu, J Li, et al., "A new hybrid filter based on differential current control method for low-order harmonic suppression in Tokamak power system," *Int J Energy Res*. vol. 42, no. 1, pp. 82-90, Jan. 2018.

[10] M. Sharanya, B. Banakara and M. Sasikala, "Power quality improvement using a combination of hybrid active power filter and thyristorised controlled reactor," *2017 International Conference on Energy, Communication, Data Analytics and Soft Computing (ICECDS)*, Chennai, 2017, pp. 1364-1369.

[11] H. Ge, Y. Zhen, Y. Wang, et al., "Research on LCL filter active damping strategy in active power filter system," *2017 9th International Conference on Modelling, Identification and Control (ICMIC)*, Kunming, 2017, pp. 476-481.

[12] Z Chen, Q Chu, "Wideband fully tunable bandpass filter based on flexibly multi-mode tuning," *IEEE Microw. Compon. Lett.* vol. 26 no. 10 pp. 789-791 Oct. 2016.

[13] J Cai, W Qin, J Chen, et al., "Novel varactor-tuned coupling mechanism and its applications to high-order bandwidth-agile bandpass filters," *IEEE Trans. Compon. Packag. Manuf. Technol.* vol. 7 no. 2 pp. 246-253 Feb. 2017.

[14] E. Rodriguez-diaz, F. D. Freijedo, S. Member, et al., "Analysis and Comparison of Notch Filter and Capacitor Voltage Feedforward Active Damping Techniques for LCL Grid-Connected Converters," *IEEE Transactions on Power Electronics*, vol. 34, no. 4, pp. 3958–3972, 2019.

[15] C. Tseng, S. Member, and S. Pei, "Stable IIR Notch Filter Design with Optimal Pole," *IEEE Transactions on Signal Processing*, vol. 49, no. 11, pp. 2673–2681, 2001.